2.1 A 24×16 CMOS-Based Chronocoulometric DNA Microarray

Marcin Augustyniak[1,3], Christian Paulus[2], Ralf Brederlow[1], Norbert Persike[4], Gerhard Hartwich[4], Doris Schmitt-Landsiedel[3], Roland Thewes[1]

[1]Infineon Technologies, Munich, Germany
[2]Siemens, Munich, Germany
[3]Technical University of Munich, Munich, Germany
[4]Friz Biochem, Munich, Germany

CMOS-based DNA microarrays utilizing electrochemical detection principles have attracted a huge amount of interest for applications in biotechnological research and medical diagnostics, since they avoid expensive and relatively bulky optical setups used in most state-of the art DNA microarray systems [1]. Moreover, they provide synergy to and easy adaptation of techniques to electrically control immobilization of DNA probe molecules, in-situ synthesis of DNA probe molecules, or stringency during hybridization [2].

DNA mircoarrays detect hybridization between single-stranded DNA target molecules in a sample and single-stranded DNA probe molecules with known sequences immobilized on predefined sites within an array. Successful binding reveals complementary matching of probe and target strands and leads to double-stranded DNA at the respective sensor sites.

Chronocoulometric DNA detection assays are based on oxidation or reduction of label molecules usually attached to the hybridized DNA target strands (Fig. 2.1.1), i.e. electron exchange between electrode and label molecule, when the potential between electrode and electrolyte is changed step-like [3,4]. Known drawbacks of such methods are background and offset signals coming from electrochemical agents in the sample solution and from the relatively huge electrode-to-electrolyte double layer capacitance. Effective measures to lower the impact of these parasitic effects are:

(1) Use of a *Differential Measurement Technique* evaluating the difference between the signals from an electrode functionalized with probe molecules of interest and an associated replica electrode, which provides a reference signal. There, the replica electrode contains receptor molecules which guarantee mismatch concerning all targets in the sample.
(2) *Fast Integration*, i.e. use of short time slots for oxidation/reduction voltage step and current integration window on the order of 1µs. In that way the amount of ions in the bulk of the electrolyte experiencing sufficient time to diffuse to the electrode is kept negligibly small.
(3) Electrochemical *Assay Optimization*, e.g. by optimizing the value of electrode-to-electrolyte voltage step to trigger the electrochemical procedure.

The sensor presented here is designed to address the three aforementioned measures. It contains an array of 24×16 working electrodes (WE) grouped in 12×16 differential pixels and a potentiostat system controlling the electrolyte potential by sensing its value through reference electrode (RE) and adjusting it through counter electrode (CE) (Fig. 2.1.2). During the measurement WEs are held at a constant potential VCM, while the electrolyte voltage changes step-like. The resulting charge is collected by an integrator circuit within the pixel.

The purpose of switch S3, connecting WEs to VCM (Fig. 2.1.2), is to fix the WE potential at VCM during readout. Moreover, it reduces the leakage current of switch S2 and makes it signal independent. The value of the leakage current, calculated on the basis of the measured drift of the output voltage during READOUT amounts to 0.14fA only.

The fully-differential pixel integrator facilitating the *Differential Measurement Technique* requires an input common mode feedback (Fig. 2.1.3) to keep WEs at VCM during INTEGRATION and READOUT. Compared with the pseudo-differential architecture used in [5] it has the advantage that for the same grade of accuracy the active area of the required operational transconductance amplifiers can be significantly reduced. The integrator op-amp (Fig. 2.1.3) accommodating differential and common-mode loops uses a folded-cascode topology with approximately rail-to-rail output voltage swing.

Double sampling is implemented by performing RESET-INTEGRATE-READOUT cycles two times, one cycle without and the other one with electrolyte voltage step, so that errors like pixel offset and switch charge injection are cancelled. The accuracy of the charge measurement can be further increased by readout noise averaging and application of calibration techniques to compensate for effective area variation of WEs.

A rail-to-rail input/output op-amp topology is used for the potentiostat, because it maximizes the freedom to choose the step potentials VIN0 and VIN1 (cf. Fig. 2.1.2) for *Assay Optimization*. In the implementation (Fig. 2.1.4) the sum of tail currents of p- and n-MOS-input differential pairs is held constant. Following [6], for proper operation input transistors are biased in weak inversion.

The chip is fabricated using a 0.5µm, 5V, 3M+2P CMOS technology extended by sensor electrodes made of gold [7]. A chip micrograph is given in Fig. 2.1.7; the entire chip area is approximately 25mm^2. To evaluate the *Fast Integration* property and the stability of the potentiostat, feedback through CE, electrolyte, and RE (cf. Fig.2.1.2) is analyzed. As a result, the electrode and the entire array layout (cf. Fig. 2.1.7) minimizes R_{RC} and maximizes R_{RW} / R_{RC}. Measurements of the dependence of the potentiostat step response on the concentration of the electrolyte (Fig. 2.1.5) confirm part of this feedback analysis, namely that low R_{RC} helps to keep the loop stable.

In Fig. 2.1.6, the result of an electrochemical experiment used for assay optimization purposes is presented. It shows the measured dependence of integrated charge (for a 100mV voltage step) on the potential between RE and VCM before the step. Electrodes with Osmium marker labeled DNA clearly provide a different answer as compared to the electrodes, which are not functionalized. Moreover, the optimum operating condition (here: V_low = -20mV) can be clearly derived.

References:
[1] M. Schena ed., "DNA Microarrays: a Practical Approach," *Oxford University Press Inc.*, Oxford, UK, 2000.
[2] P. Caillat et al., "Biochips on CMOS: an Active Matrix Address Array for DNA Analysis," *Sensor and Actuators B*, vol. 61, pp.154-162, 1999.
[3] A. J. Bard and L. R. Faulkner, "Electrochemical Methods," *John Wiley & Sons, Inc.,* 2001
[4] C. Paulus et al., "A Fully Integrated CMOS Sensor System for Chronocoulomety," *Proc. IEEE Sensors,* pp. 1329-1332, 2003.
[5] A. Hassibi et al., "A Programmable Electrochemical Biosensor Array in 0.18µm Standard CMOS," *ISSCC Dig. Tech. Papers,* pp. 564-565, Feb., 2005.
[6] J. H. Huijsing et al., "Low-Voltage Operational Amplifier with Rail-to-Rail Input and Output Ranges," *IEEE J. Solid State Circuits*, vol. 20, no. 6,, pp.1144-1150, June, 1985.
[7] F. Hofmann et al., "Fully Electronic DNA Detection on a CMOS Chip: Device and Process Issues," *Tech. Dig. IEDM*, pp. 488-491, 2002.

 1-4244-0079-1/06/$20.00

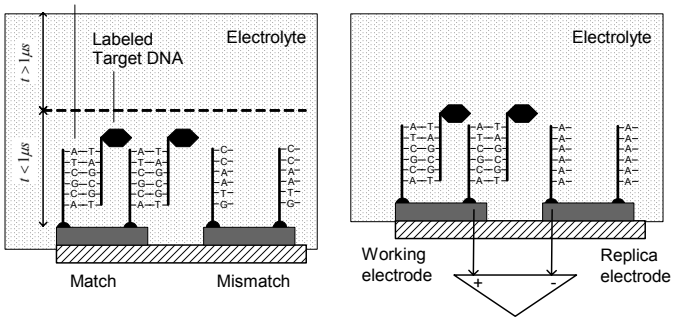

Figure 2.1.1: Sensor principle including schematic description of relevant time constants (left), differential readout configuration (right).

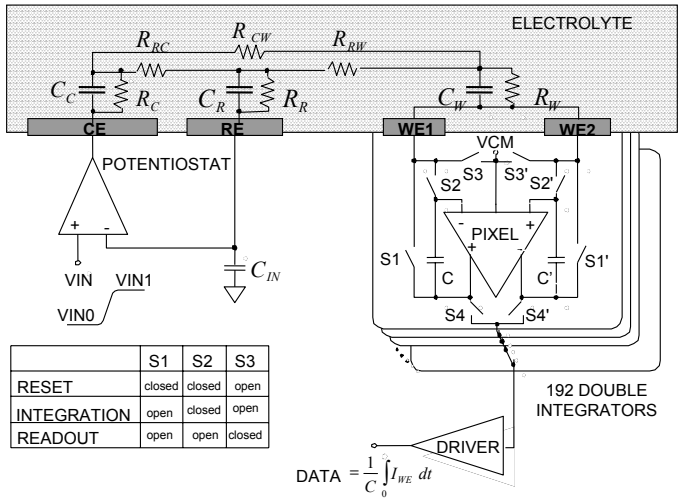

	S1	S2	S3
RESET	closed	closed	open
INTEGRATION	open	closed	open
READOUT	open	open	closed

Figure 2.1.2: Chip architecture and electrolyte equivalent circuit.

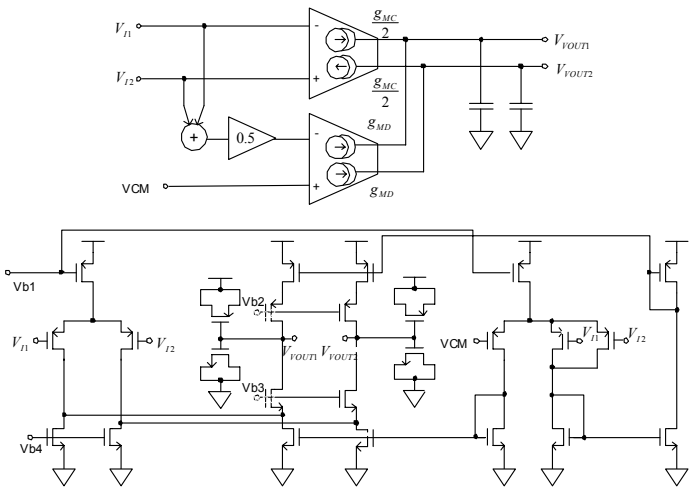

Figure 2.1.3: Concept and transistor-level implementation of pixel opamp with input CMFB circuit.

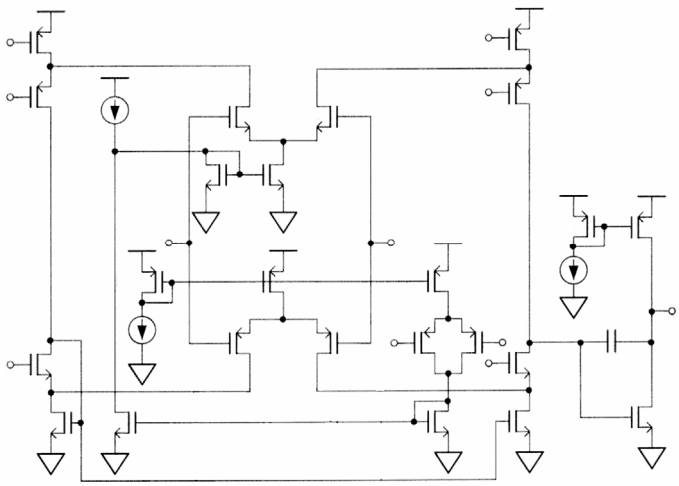

Figure 2.1.4: Schematic of rail-to-rail potentiostat opamp.

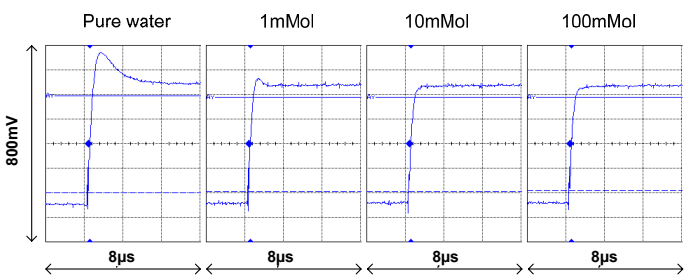

Figure 2.1.5: Step response of the potentiostat for different electrolyte concentrations.

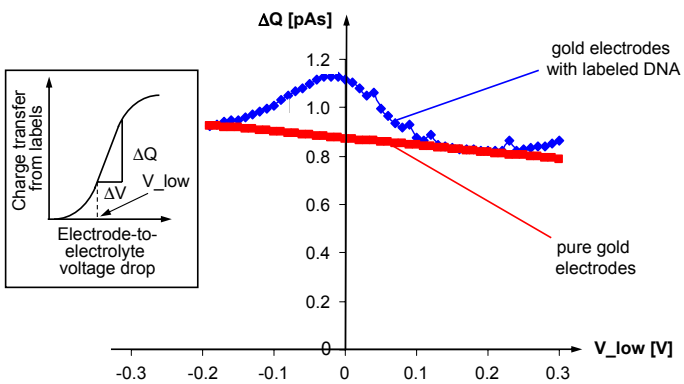

Figure 2.1.6: Transferred charge ΔQ at a voltage step ΔV=100 mV as a function of V_low. Inset: Setup. Main figure: Measured data from gold electrode w/wo labeled DNA.

Continued on Page 636

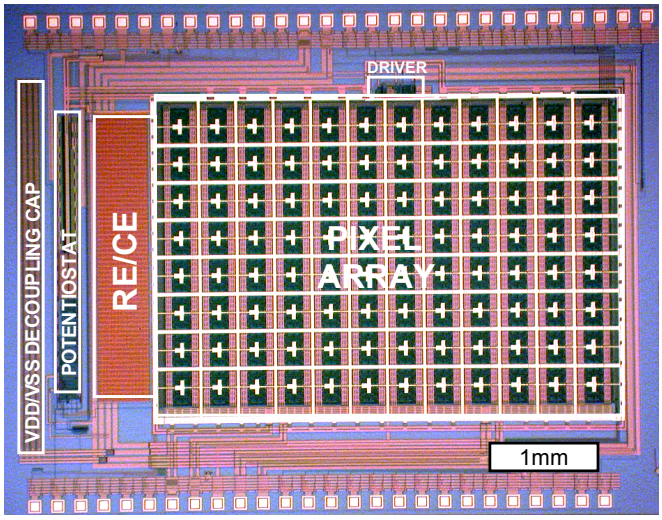

Figure 2.1.7: Chip micrograph.

